Mossbauer spectroscopy investigations of the oxidation of alpha $_2$-Sn and beta -Sn types of structure at room temperature

1994 J. Phys.: Condens. Matter 6 2083

(http://iopscience.iop.org/0953-8984/6/10/026)

J. Phys.: Condens. Matter 6 (1994) 2083–2092. Printed in the UK

Mössbauer spectroscopy investigations of the oxidation of α_2-Sn and β-Sn types of structure at room temperature

S K Peneva†, N S Neykov†, V Rusanov‡ and D D Chakarov§

† University of Sofia, Department of Physical Chemistry, 1 James Bourchier Avenue, Sofia 1126, Bulgaria

‡ University of Sofia, Department of Atomic Physics, 5 James Bourchier Avenue, Sofia 1126, Bulgaria

§ Bulgarian Academy of Sciences, Institute of General and Inorganic Chemistry, Sofia 1040, Bulgaria

Received 6 July 1993, in final form 25 October 1993

Abstract. *The initial oxidation of two groups of tin structures with different chemical bindings,* designated as α_2-Sn type and β-Sn type, simultaneously grown by different electrochemical reductions is investigated by Mössbauer spectroscopy, and partly by x-ray photoelectron spectroscopy. It is shown that during the growth process the tin types become oxidized either to a mixture of tin(II) and tin(IV) oxides, or to tin(IV) oxides, but that the later oxidation in air at room temperature, monitored by periodic Mössbauer studies, is always to tin(IV) oxides. The kinetic results show that the mechanisms of oxidation of the two tin types are almost identical and that, if there is some difference, as suggested by parallel electron diffraction studies, it is beyond the sensitivity of the method. The oxidation of the tin types is a two-stage process, with a very large initial rate of oxidation, which decreases after aging for 1 or 2 months. Numerical equations describing parts of the oxidation curves are derived. The influence of impurities on the oxidation process is discussed.

1. Introduction

The initial oxidation of two groups of coexisting tin structures (tin types), with different chemical bindings, grown by different electrochemical reductions is analysed by Mössbauer spectroscopy (MS), and in some cases by x-ray photoelectron spectroscopy (XPS). It is shown that it depends on the particular growth process. The MS studies show that their later oxidation in air at room temperature is always to tin(IV) oxides. The initial and the later oxidation of the tin products grown by reduction of water solutions of $SnCl_2$ or $SnSO_4$ with Mg are especially analysed, since that information is important for characterization of the unusual tin types after the growth process, and during aging at room temperature (see, e.g. [1, 2]). The oxidation is investigated by monitoring the changes in the Mössbauer spectral line intensities within an interval of approximately two years.

The two tin types are defined by the values of the isomeric shifts δ of their Mössbauer lines, and are designated as

(a) α_2-Sn type and
(b) β-Sn type [1].

(a) The α_2-Sn type includes tin states different from the known α-Sn and β-Sn [3]. More details are included in [4–6] for the case of thin films, and the existence of these structures in the macroscopic state [1, 2, 7, 8]. The α_2-Sn type possesses unusually high

0953-8984/94/102083+10$19.50

values of δ, explained by the eventual participation of d electrons in their chemical bindings [6].

(b) The β-Sn Mössbauer line also has a complicated substructure [8]. Tin crystalline states with isomeric shifts close to that of β-Sn are defined as β-Sn type (the theoretical value of δ for β-Sn is $+2.65$ mm s^{-1} [9]). β-Sn and the 'excited β-Sn' structures [10] are, so far, the known tin structures belonging to the β-Sn type.

The oxidation of both tin types is compared with kinetic and spectroscopic data of low-temperature oxidation of thin tin films and tin foils (see, e.g. [11–15]).

2. Experimental details

α_2-Sn and β-Sn types are obtained by reducing 20% aqueous solutions of $SnCl_2$, (experiments (products) A–D) or of $SnSO_4$ (experiment (product) E) with Mg at room temperature; more details concerning the reduction procedures have been included in [1, 2]. There are intentionally introduced differences in the initial state of the aqueous solutions of $SnCl_2$. The solutions of A–C are not filtered before performing the reductions and contain more products of the $SnCl_2$ hydrolysis than does the solution of D, which is filtered by a membrane Millipore Millex-GV 0.22 μm filter unit; NH_4Cl is added to the $SnCl_2$ solution of C to minimize the process of hydrolysis. All reagents have an analytical grade of purity. The precipitates obtained are rinsed several times with distilled water and are dried in air.

The reduction product R is obtained by adding solid $SnCl_4.5H_2O$ to a 5% aqueous solution of $NaBH_4$. The pH should be 10–11; this is obtained and maintained by adding solid NaOH to the reaction system. Continuous electromagnetic stirring during the reaction leads to formation of a metallic-looking ball at the bottom of the reaction system: R (lower fraction). R (upper fraction) consists of particles suspended in the reaction system.

XPS investigations, performed on an ESCALAB II (VG) electronic spectrometer, give integral information of the chemical composition, and the impurity contents of the layers approximately 50 Å thick of each product. Tablets of the respective material are degassed at room temperature up to 1×10^{-10} Torr. Monochromated Mg Kα radiation ($h\nu = 1253.6$ eV) is used. The binding energies are referred to the C 1s position. The instrumental resolving power is 1.0 eV. The observed charging effects are evaluated but not compensated. The recording of all photoelectron spectra is performed under identical experimental conditions. Computer fitting is used to process the experimentally observed spectra.

Periodically performed selected-area electron diffraction (SAD) studies in a TESLA BS 540 electron microscope working at 80 kV give information on the changes with time, and the oxidation of the various tin structures (see, e.g. [1, 10]). Information concerning the state of the undesired impurities is obtained also with a Philips TEM 420/EDAX instrument.

At particular time intervals t, a defined quantity of each precipitate is weighed and is investigated by Mössbauer spectroscopy. A standard Mössbauer spectrometer with a 5 mCi $^{119m}BaSnO_3$ source is used. All spectra are computer fitted, and the spectral lines of the α_2-Sn and the β-Sn types are resolved into single Lorentzians. More details have been given in [2].

3. Experimental results and discussion

3.1. Characterization of the as-grown tin products

The Mössbauer spectra of the products A–E recorded after their respective reductions are similar but show a variation in the spectral line intensities. The products are mixtures

of α_2-Sn type, β-Sn type and tin(IV) oxides, and microquantities of amorphous tin(II) oxides (figure 1) [1, 2, 8]. The product R (upper fraction) consists of tin(IV) oxides, and microquantities of α_2-Sn type and β-Sn type; R (lower fraction) consists of β-Sn type and tin(IV) oxides (figure 2).

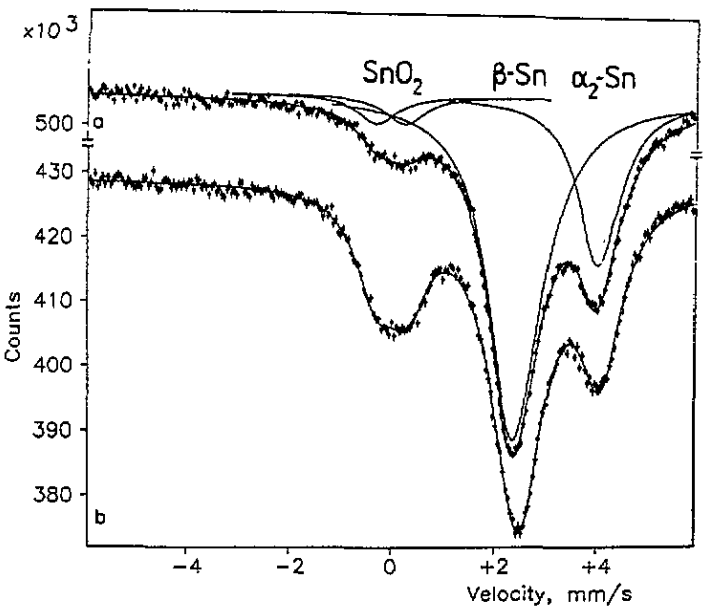

Figure 1. Mössbauer spectra from the reduction product D: curve a, recorded after the reduction; curve b, recorded after exposure to air for 4.5 months at room temperature.

XPS results of several independently performed reductions of $SnCl_2$ with Mg show that there is almost no impurity such as Mg in the products of types A–D, but that they contain a considerable quantity of chlorine. Microquantities of at least four chlorine-containing tin compounds ([Cl]/[Sn] molecular ratios of the order of 2/3, 1/3 and 3/4 are detected by SAD using a Philips TEM 420/EDAX electron microscope). Their existence is connected with gradual substitution of chlorine ions by OH groups, since the pH inside the reaction system increases during the reaction [16] (initial pH approximately 2). Two of these compounds, namely those with [Cl]/[Sn] ratios of 2/3 and 1/3, which are probably pseudo-hexagonal, with relatively large lattice parameters (a in the range 9–10 Å and c of the order of 7–8 Å) are identical with those of the SnO_2–VI series, introduced in [1], a fact which permits us to rule out the existence of another SnO_2 series in the products of reduction of $SnCl_2$ with Mg.

The presence of microquantities of chlorine-containing compounds on the surfaces of both tin types in the products A–D is expected, despite the fact that it is not revealed by energy-dispersive x-ray analysis (EDXA) studies.

Sulphur-containing microparticles are found by EDXA in the product E. Microcontaminations of sulphur on the tin surfaces should also not be excluded.

There is neither boron nor chlorine in the two fractions of the reference product R (table 1).

The chemical state of tin in the initial oxides grown during the reductions cannot be determined by the shifts in the binding energy of the $3d_{5/2}$ electrons, since the chemical

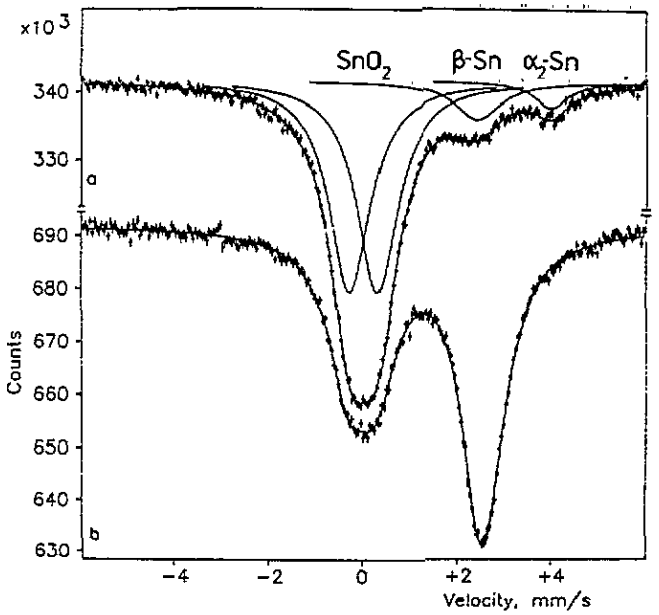

Figure 2. Mössbauer spectra of R (upper fraction) (curve a) and R (lower fraction) (curve b) obtained after reduction of $SnCl_4$ with $NaBH_4$.

shifts in the 3d levels of SnO and SnO_2 are very close [13, 17]. The valence band structure of tin here is complicated and is not suitable for characterization of the tin surfaces as for example in [13]. Information on the stoichiometry of the observed oxides is derived from the [Sn]/[O] ratio. The interpretation of this ratio is influenced by the partial reduction of SnO_2 to SnO, and Sn by the electron or photon irradiation in vacuum [18], but that effect is not taken into account in the present analysis. The XPS results show that the reaction products of $SnCl_2$ with Mg, as do products A–D, contain a mixture of tin(II) and tin(IV) oxides, but that the reference product R contains stoichiometric SnO_2 (theoretical [Sn]/[O] ratio 0.5) (table 1).

The XPS results (table 1) show that one of the possible mechanisms of initial oxidation of tin is to tin(II) and tin(IV) oxides, i.e. the oxidation of products A–D grown by reducing $SnCl_2$ with Mg. This result is in accordance with the high-resolution Mössbauer spectroscopy data [8]. The other oxidation mechanism is to tin(IV) oxides only. It takes place during the initial oxidation of the products R, grown by the reduction of $SnCl_4$, with $NaBH_4$.

Parallel SAD investigations of the products R show that the initial oxides there are either amorphous or $An^{V}O_2$ [1]. So, the Mössbauer results in [1], suggesting the tetravalent state of tin in SnO_2–V are confirmed by the XPS data of the present study.

There is no common opinion on the valence state of tin in the tin oxides grown at low temperatures onto different tin surfaces. Mixtures of tin(II) and tin(IV) oxides are observed by ESCA on tin films heated at 100 °C in an O_2 atmosphere [13], and by depth-selective Mössbauer spectroscopy (DSMS) on tin films heated at 200 or 300 °C in air [12]. UPS observations show that the oxidation of thin tin films at room temperature is to tin(IV) oxides [19]. Lau and Wertheim [13] explain the growth of the tin(IV) oxides observed in [19] as growth on top of the SnO already grown. This model is in contradiction to DSMS and electron diffraction data in [12], which show that both types of oxide coexist side by side

Table 1. XPS data from products R (reduction of $SnCl_4$ with $NaBH_4$), compared with similar data registered from products of the type D (reduction of $SnCl_2$ with Mg). Traces means less than 0.5%.

	Experimentally determined binding energy E_b (eV) (C 1s ≡ 285.0 eV)			Charging energy
Sample	$Sn^{(0)}$ $3d_{5/2}$	$Sn^{(II-IV)}$ $3d_{5/2}$	O 1s	(eV)
R (lower)	484.45	486.65	530.55 531.25	0.85
R (upper)		486.80	531.15	4.85

	Chemical state of Sn (%)		
Sample	Sn(0)	$Sn^{(II-IV)}$	$[Sn^{(II-IV)}]/[O]$
R (lower)	11.0	89.0	0.51
R (upper)	Traces	100.0	0.53

	Composition (at.%)		
Sample	Sn	O	Remark
R (lower)	36.5	63.5	Cl, B, traces
R (upper)	34.6	65.4	Cl, B, traces

Sample of	Composition (at.%)			[Sn]/[O][a]
type D	Sn	O	Cl	ratio
1	43.83	45.35	10.82	0.85
2	41.85	43.48	14.67	0.79
3	41.10	46.76	12.14	0.75

[a] It is assumed that all chlorine atoms are in the form of $SnCl_2$; the samples contain traces of Mg (less than 0.5%).

on the oxidized tin surface and inside the as-grown oxide layers. The results of the present study show that the oxidation of tin can take place by both mechanisms. It is considered that the growth of tin(II) or tin(IV) oxides is somehow connected to the presence of different metastable tin structures [1, 4, 6, 8, 10].

Data have shown that the initial thickness of the oxides on some tin types is less than 50 Å (see for example the presence of metallic tin $Sn^{(0)}$ in the R (lower fraction) (table 1)). Similar observations exist for some samples of type A–D. The presence of metallic tin is not observed in all XPS data, an indication that the initial oxide thicknesses on the different tin types are different.

3.2. Secondary oxidation in air at room temperature; analysis of the Mössbauer results

The Mössbauer results show that the oxidation in air at room temperature of all reduction products gives tin(IV) oxides (see for example, figure 1). The time intervals of monitoring the changes in samples A–C are relatively large. The changes in samples D and E are recorded at short time intervals, so as to obtain more detailed information of the initial stages of oxidation of the two tin types.

Some preliminary data on the changes in the isomeric shifts δ, the quadrupole splittings Δ and the areas of the Mössbauer lines of samples A–C, recorded over a period of one and a half years, have been reported in [1]. There it is demonstrated that the values of δ and Δ of the Mössbauer lines of the three components: β-Sn type, α_2-Sn type and SnO_2 remain almost the same during that time period, but that the relative areas S_i of the Mössbauer

lines change. Here $i = 1$ represents the β-Sn type, $i = 2$ the α_2-Sn type and $i = 3$ the line of SnO_2. Each S_i is defined as the area of the ith line divided by the total area of all lines. S_1 and S_2 decrease during aging, while S_3 increases.

The kinetic studies require the absolute values of the quantities $d_{i,t}$ of the changing substances (t is the time in days after the reduction). Relative values, referred to the quantity of β-Sn type, are used in the later calculations, since the absolute values are not easily determined. At $t = 0$ they are

$$d_{2,0}/d_{1,0} = (f_1'/f_2')(S_{2,0}/S_{1,0}) \qquad d_{3,0}/d_{1,0} = (f_1'/f_3')(S_{3,0}/S_{1,0}). \tag{1}$$

$S_{i,t}$ is the area of the spectral line of the ith component at time t. The values of the factors f' are considered to be $f_1' = f_2' = 0.05$, for the β-Sn and α_2-Sn types and $f_3' = 0.5$ for SnO_2. These assumed values are close to the experimentally determined f'-values of the respective substances at room temperature [9]. The basic conclusions of the present analysis are not altered substantially by the inaccuracies introduced by this assumption. The following considerations favour equations (1).

(i) The effective thickness of the samples is in the linear part of the absorption for all three components.

(ii) The largest value of the relation $\epsilon = \Delta N/N_\infty$ is less than 0.12–0.13 (ΔN is the absorption at the maximum of the line; N_∞ is the intensity of the recorded radiation outside the resonance absorption).

The relation

$$\eta_{i,t} = (d_{i,t}/d_{1,t})/(d_{i,0}/d_{1,0}) = (S_{i,t}/S_{1,t})/(S_{i,0}/S_{1,0}) \tag{2}$$

is introduced, to avoid effects due to the uncontrolled changes in sample thicknesses.

The Mössbauer data obtained from samples from different experiments show that the values of the spectral lines areas S of the β-Sn type and the α_2-Sn type, referred to a unit time necessary to record a spectrum, decrease negligibly with time (starting from $t = 0$). This is not so for the area of the SnO_2 line, which increases rapidly, and is three to four times the initial area at the end of the experiment. An illustration of the former statement, described by the parameter η, is included in figure 3.

The following conclusions can be drawn from the above analysis.

(i) The rates of oxidation of the β-Sn type and of the α_2-Sn type are almost the same, if the relative contents of both types remain unchanged (figure 3).

(ii) Initially, the quantity of SnO_2 increases rapidly, but later it shows a tendency towards saturation. The fact that small changes in the quantities of β-Sn type and α_2-Sn type lead to considerable changes in the SnO_2 spectral line area can be easily understood by considering the f'-value of SnO_2, which is about ten times the f'-values of the two Sn types.

The kinetics of oxidation of tin are described by considering the changes, with time, in the SnO_2 quantity.

The quantity $d_{1,t}$ of β-Sn type and the quantity $d_{3,t}$ of SnO_2 after a time interval t are defined by assuming that the relative change in the quantities of β-Sn type and of α_2-Sn type are identical, and by defining this relative change as $\delta_t = \Delta d_t/d_0$:

$$d_{1,t} = p_t d_{1,0}(1 - \delta_t) \tag{3}$$

$$d_{3,t} = p_t[d_{3,0} + \delta_t(d_{1,0} + d_{2,0})]. \tag{4}$$

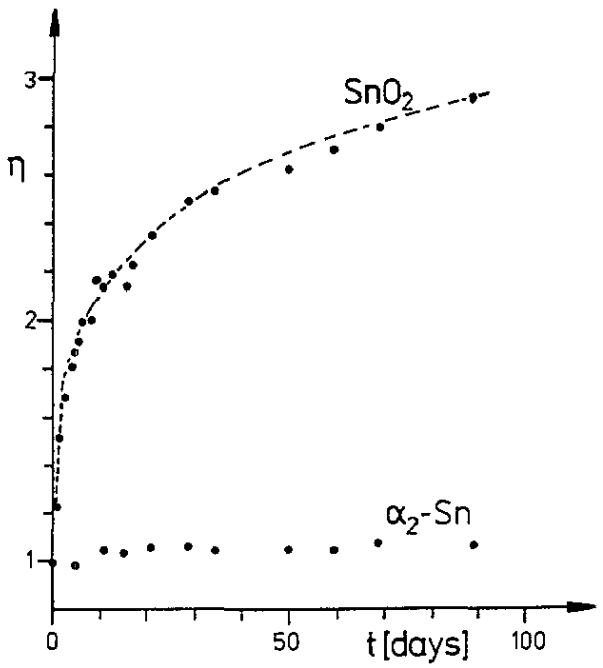

Figure 3. Typically observed relative change in the α_2-Sn type and SnO_2 quantities, described by the time dependence of the parameter η (equation (2)).

Here p_t is the ratio of the total thickness of the sample at time t referred to that at time $t = 0$. The following relation is derived after assuming, for simplicity, that $d_{1,0} = 1$:

$$\eta_{3,t} = [1/(1 - \delta_t)][1 + \delta_t(1 + d_{2,0})/d_{3,0}] = (S_{3,t}/S_{1,t})/(S_{3,0}/S_{1,0}). \tag{5}$$

δ_t is obtained from the experimentally determined values of $S_{i,t}$:

$$\delta_t = (\eta_{3,t} - 1)/(k - \eta_{3,t}) \tag{6}$$

where

$$k = (1 + d_{2,0})/d_{3,0}. \tag{7}$$

The value of δ_t corresponds to the quantity of β-Sn plus α_2-Sn types, which has transformed itself into SnO_2, after a time interval t. δ_t is proportional to the thickness of the SnO_2 surface layers grown on both tin types, and its dependence of t can be described by

$$\delta_t = at^b. \tag{8}$$

Here a and b are constants. Figure 4 illustrates the validity of this law for the samples A–E. The values of a and b are calculated from the linear parts of the functions, and the results obtained are included in table 2. Table 2 contains also values of $d_{2,0}$ and of $d_{3,0}$ calculated from equation (1) by assuming that $d_{1,0} = 1$.

All experiments show a very rapid initial increase in the oxide layer thickness (figure 4). A linear dependence could be fitted for the initial data of experiment D (there are fewer data for products A–C) but not to similar data for product E (grown by reducing $SnSO_4$).

Table 2 shows the following.

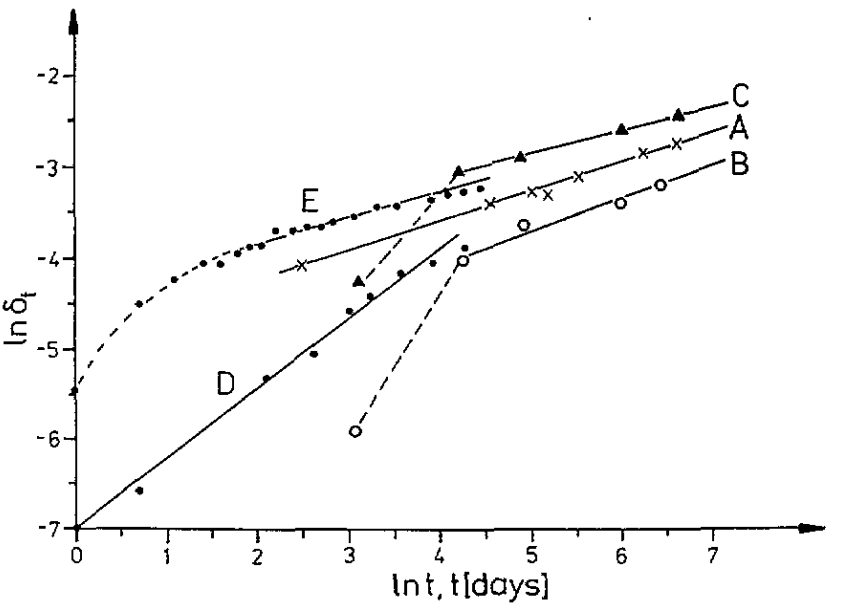

Figure 4. Oxidation of the α_2-Sn plus β-Sn types to SnO_2 at room temperature. Samples A–D are grown by reduction of $SnCl_2$ with Mg. Sample E is obtained by reducing $SnSO_4$ with Mg.

Table 2. Initial quantities $d_{2,0}$ of the α_2-Sn type and initial quantities $d_{3,0}$ of SnO_2 in the products A–E, calculated from equation (1), by assuming the initial quantity of the β-Sn type to be $d_{1,0} = 1$. The values of the constants a and b (equation (8)) are also included. t_{max} [days] shows the time of observation of each sample.

Sample	$d_{2,0}$	$d_{3,0}$	a	b	t_{max} (d)
A	0.22	0.063	0.0080	0.30	737
B	0.38	0.066	0.0052	0.31	613
C	0.30	0.060	0.019	0.22	722
D	0.39	0.013	0.0010	0.76	71
E	0.33	0.027	0.018	0.17	89

(i) The relative quantity of the α_2-Sn type, referred to that of the β-Sn type, varies within a relatively small interval, despite the differences in the reduction systems.

(ii) The initial quantities of SnO_2 are comparable.

(iii) The value of b between 1 and 1/2, obtained for the initial oxidation stage in experiment D, suggests that the initial oxidation of tin depends both on the surface conditions and on the diffusion mechanism(s) through the as-grown oxide layers [20].

(iv) The values of b for the second stage of oxidation of products A and B define a cubic rate law. A fourth-power rate law is valid for the product C.

(v) The value of b calculated for the second stage of oxidation of product E (containing sulphur microparticles) is the lowest and defines approximately a fifth-power rate law. The initial rate of oxidation of this product is the largest (figure 4).

Kinetic results on oxidation of tin foils in air at room temperature, summarized for example in [15], show that there are differences between the data in the literature; some workers report a law linear with the oxidation time, in contradiction to the generally agreed

logarithmic rate of oxidation. Growth tends to be parabolic above 130 °C and better around 200 °C. The complicated rate laws observed in the present study depend most probably on the impurities present on the tin surfaces, such as water and some chlorine- or sulphur-containing compounds. Tin(II) chloride hydroxides and SnS are reported to possess some passivation effects [15]. A similar effect is observed for NH_4Cl (product C). The present results show that the largest passivation of the tin surfaces is in the presence of sulphur or sulphur-containing compounds (table 2).

The observed two-stage oxidation of the tin types in air at room temperature (figure 4) is in accordance with the parallel SAD observations. There is considerable initial instability of the tin structures in the various reduction products, which decreases after aging for several months [1]. The relative decrease in the instability of both tin types is associated with the beginning of the second stage of the oxidation process and with the appearance of cassiterite on the surfaces of some tin crystallites.

The oxides on some α_2-Sn type samples remain amorphous even after aging for about two years, and their presence does not hinder the SAD investigations. The structure of tin crystals covered with cassiterite cannot be investigated by SAD. This suggests some difference in the oxidation process, at least for some of the α_2-Sn type. The results of the present study show that this difference is beyond the sensitivity of the conventional Mössbauer spectroscopy investigations.

The valence state of tin in the growing oxides considered here is always under control. This is not so for kinetic investigations where the valence state of tin is deduced from x-ray or electron diffraction data (see, e.g., [11, 14]). The growing oxides can show a deviation from crystallinity, as in the present case (see also [1]), and this is not recorded in the x-ray diffraction studies. The electron diffraction powder data from an oxidized tin surface can be very complicated [14], and their interpretation as α-SnO is ambiguous [13].

4. Conclusions

The oxidation in air at room temperature to tin(IV) oxides of two groups of tin structures, α_2-Sn type and β-Sn type, is observed by Mössbauer spectroscopy. These results are obtained during parallel SAD observations of the structural changes of the tin types during aging (see, e.g., [1, 2]). The tin types are grown by different electrochemical reductions; they are oxidized during the growth itself and contain different impurities. The valence state of the initially grown oxides, and the nature of the impurities are analysed by XPS, and partially by EDXA. The system is complicated, but it gives a unique opportunity to study simultaneously the structural changes and the kinetics of oxidation of two groups of allotropic forms of a metal, with very different chemical bindings. In this system the two tin types exist side by side, but not at different depths as is the case for a thin tin film [4].

It is shown that the initial oxidation of tin in the different reduction systems is either to a mixture of tin(II) and tin(IV) oxides, or to tin(IV) oxides only.

The analysis of the Mössbauer data shows that there is almost no difference between the mechanisms of the later oxidation of both tin types. Arguments based on SAD observations are presented which suggest that such a difference exists, but it is beyond the sensitivity of the present types of investigation.

The Mössbauer data show that the initial rate of oxidation in air of both tin types is very large and depends both on the surface conditions and on the diffusion through the as-grown oxide layers. The SAD observations described partly in [1] relate the enhanced initial rate of oxidation to the considerable initial structural instability of some of the metastable tin

structures. The beginning of the lower oxidation stage is associated with the formation of cassiterite on the surfaces of some tin types.

Cubic, quadratic and even fifth-power oxidation laws are derived. The complicated rate equations are associated with the presence of impurities, and their passivation effects.

The XPS data of the reference product R (table 1) confirm the Mössbauer results in [1] of the tetravalent state of tin in SnO_2–V. This oxide grows at room temperature on some α_2-Sn films [21].

Acknowledgments

The authors are highly grateful to Dr D D Nihtianova for the Philips TEM 420/EDAX observations.

References

[1] Peneva S K, Neykov N S, Djuneva K D and Rusanov V 1992 *Z. Kristallogr.* **202** 191
[2] Rusanov V, Bonchev Ts, Peneva S K, Chakarova K H, Spasov L A and Petrov S L 1984 *J. Solid State Chem.* **51** 336
[3] *Powder Diffraction File* 1988 (Swarthmore, PA: International Center for Diffraction Data)
[4] Peneva S K and Djuneva K D 1984 *Thin Solid Films* **113** 297
[5] Tsukeva E A, Tsakin E, Peneva S K and Djuneva K D 1989 *Z. Kristallogr.* **187** 63
[6] Bonchev Ts, Peneva S K and Djuneva K D 1981 *Kinam* **3** 389
[7] Rusanov V, Bonchev Ts, Mandjukov I and Mihov M 1986 *J. Phys. F: Met. Phys.* **16** 515
[8] Rusanov V, Mandjukov I, Bonchev Ts and Kantchev K 1988 *J. Phys. F: Met. Phys.* **18** 1311
[9] Goldanskii V I and Herber R H (ed) 1968 *Chemical Applications of Mössbauer Spectroscopy* (New York: Academic)
[10] Neykov N S, Peneva S K and Djuneva K D 1992 *Z. Kristallogr.* **202** 215
[11] Nagasaka M, Fuse H and Yamashina T 1978 *Thin Solid Films* **29** L29
[12] Chan Duk Thiep, Bonchev Ts, Nguyen Chi Toa and Peneva S K 1977 *Bulg. J. Phys.* **4** 399
[13] Lau C L and Wertheim G K 1978 *J. Vac. Sci. Technol.* **15** 622
[14] Boggs W E, Kachik R H and Pellissier G E 1961 *J. Electrochem. Soc.* **108** 6
Boggs W E, Trozzo P S and Pellissier G E 1961 *J. Electrochem. Soc.* **108** 13
Boggs W E 1961 *J. Electrochem. Soc.* **108** 124
[15] Gabe D R 1977 *Surf. Technol.* **5** 463
[16] Ichida S and Takeshita M 1984 *Bull. Chem. Soc. Japan* **57** 1087
[17] Briggs D and Seach M P (ed) 1983 *Practical Surface Analysis by Auger and X-ray Photoelectron Spectroscopy* (New York: Wiley) pp 567–90
Wagner C D, Riggs W M, Davis L E, Moulder J F and Muilenberg E E (ed) 1979 *Handbook of X-ray Photoelectron Spectroscopy* (Eden Prairie, MN: Physical Electronics Division, Perkin-Elmer Corporation)
Nefedov V I 1984 *X-ray Electron Spectroscopy of Chemical Compounds* (Moscow: Chimia) p 175 (in Russian)
[18] Edgell R G, Eriksen S and Fiavell W R 1987 *Surf. Sci.* **192** 4265
[19] Powell R A and Spicer W E 1976 *Surf. Sci.* **55** 681
[20] Lawless K R 1974 *Rep. Prog. Phys.* **37** 231
[21] Djuneva K D, Peneva S K, Tsukeva E A and Batov I 1980 *Thin Solid Films* **67** 371